SCIENTIFIC REPORTS

OPEN

SUBJECT AREAS:
MATERIALS SCIENCE
MECHANICAL ENGINEERING

Received
2 October 2014

Accepted
5 January 2015

Published
28 January 2015

Correspondence and requests for materials should be addressed to X.Y.W. (wangxy_hust@163.com)

A size-dependent constitutive model of bulk metallic glasses in the supercooled liquid region

Di Yao, Lei Deng, Mao Zhang, Xinyun Wang, Na Tang & Jianjun Li

State Key Laboratory of Materials Processing and Die & Mould Technology, Huazhong University of Science and Technology, 1037 Luoyu Road, 430074 Wuhan, Hubei, China.

Size effect is of great importance in micro forming processes. In this paper, micro cylinder compression was conducted to investigate the deformation behavior of bulk metallic glasses (BMGs) in supercooled liquid region with different deformation variables including sample size, temperature and strain rate. It was found that the elastic and plastic behaviors of BMGs have a strong dependence on the sample size. The free volume and defect concentration were introduced to explain the size effect. In order to demonstrate the influence of deformation variables on steady stress, elastic modulus and overshoot phenomenon, four size-dependent factors were proposed to construct a size-dependent constitutive model based on the Maxwell-pulse type model previously presented by the authors according to viscosity theory and free volume model. The proposed constitutive model was then adopted in finite element method simulations, and validated by comparing the micro cylinder compression and micro double cup extrusion experimental data with the numerical results. Furthermore, the model provides a new approach to understanding the size-dependent plastic deformation behavior of BMGs.

Bulk metallic glasses (BMGs) with excellent mechanical properties have become a research hotspot and promising potential as structural and functional materials[1–3]. It is suitable for manufacturing the complex precision micro- and nano-scale components due to its super-plasticity in the supercooled liquid region (SCLR)[4]. There are several interesting phenomena in the deformation process of BMGs, such as stress overshoot and steady-state stress. In order to precisely describe the deformation behavior of BMGs, many constitutive theories have been proposed in recent years. As an important physical property of BMGs, the viscosity can reflect an intrinsic resistance to atomic movement and a time scale for structural rearrangements during BMGs deformation behavior[5]. It is characterized by the relationship between flow stress σ and shear rate $\dot{\gamma}$[6].

$$\eta = \sigma/\dot{\gamma} = \sigma/3\dot{\varepsilon} \tag{1}$$

where $\dot{\varepsilon}$ is the strain rate. Kato[7] studied the relationship between the kinetic viscosity and strain rate of $Pd_{30}Ni_{10}Cu_{30}P_{20}$ BMGs in the SCLR through the compression test. Kawamura[8] reported that the strain rate dependence of viscosity can be described by a stretched exponential function and proposed the Arrhenius-type formulation of viscosity in the SCLR. Johnson[9] presented a simple self-consistent model of steady-state viscosity, namely the VFT-equation. He deemed that the viscosity is related to the generation and annihilation of free volume in BMGs, which can explain the overshoot phenomenon. Lu[10] proposed a fictive stress model in terms of structural relaxation-induced stress. The model describes the stress overshoot phenomenon under constant and multiple strain-rate loading. Through combining the stress relaxation hypothesis and fictive stress theory, Kim[11] proposed a constitutive model enables describe nonlinear viscoplastic flow deformation of Pd-based BMGs. Wang[12] proposed a Maxwell-pulse constitutive model in terms of introducing a pulse model into fictive stress model, to accurately describe both the steady-state flow behavior and the stress overshoot phenomenon of BMGs in the SCLR. Jun[13] modified the elastic–viscoplastic constitutive model proposed by Anand[14,15], which could describe the whole strain-rate dependent deformation behavior of BMGs by introducing new parameters of free volume variations. In the past few years, some research found an interesting phenomenon that deformation behavior of BMGs exhibit a strong dependence on sample size and the dependent rule presents diversity. Huang[16] claimed that $Ti_{40}Zr_{25}Ni_3Cu_{12}Be_{20}$ BMG exhibits significantly decreasing stress with size decreasing at room temperature, suggesting a 'smaller is softer' trend. However, Zheng[17] indicated that the flow stress of Mg-based

BMG increases with sample diameter decreasing in millimeter scales. In the SCLR, Li[18] reported that the compressive stress of $Zr_{65}Cu_{17.5}Ni_{10}Al_{7.5}$ BMG increases with decreasing sample size at various strain rates. Wang[19] also indicated that the smaller the specimen, the higher the flow stress will be, namely 'smaller is harder'.

The above research results show that the sample size has significant influences on deformation behavior of BMGs, namely size effect. However, this extremely important effect has not been taken into account within all of these constitutive models, which will lead deviations in accuracy of describing the deformation behavior. Hence, a constitutive model considering the size effect is necessary to be established. In the presented study, a new constitutive model with size-dependent factors based on the Maxwell-pulse type model previously presented by authors was established to accurately describe the deformation behavior of the size effect in the SCLR. At the same time, the mechanism of the size effect was discussed based on the free volume model and transition state theory.

Results

Figure 1 shows the typical true stress–strain curves of $Zr_{55}Cu_{30}Al_{10}Ni_5$ BMG with different sizes at various conditions through the micro cylinder compression. All error bars of the curves are less than 5%. It is evident that the deformation behavior is not only dependent on temperature and strain rate, but also sensitive to sample size. In Figure 1a, the values of true stress increase sharply during the initial stage of the whole deformation, which is elastic deformation stage. The slope of true stress–strain curves before a true strain of 0.02 can be defined as the elastic modulus[20]. As deformation continues, the stress reaches a peak value and subsequently declines to a relatively stable plateau, known as the stress-overshoot phenomenon. The peak value and corresponding strain are overshoot peak stress and peak strain respectively. The stable true stress is the steady stress.

It is obvious that the difference of sizes can influence on steady stress, overshoot peak stress, peak strain and elastic modulus. Under the same condition, the steady stress, overshoot peak stress and elastic modulus all increase with the sample size decreasing. On the contrary, the peak strain decreases with size decreasing. It implies that the apparent viscosity increases with the sample size decreasing in the millimeter scale. A similar phenomenon was reported in other BMGs and nano-scale[18,21]. In Figure 1b, it is interesting that the stress–strain curve of the smallest sample (Ø0.6 mm) exhibits a distinct stress overshoot under the condition of 704 K and 0.005 s^{-1}. However, the overshoot phenomenon entirely disappears in the largest sample (Ø3 mm). It indicates that there is a transition from non-Newtonian flow to Newtonian flow with size increasing.

Discussion

The free volume inside BMGs can be termed as excess volume compared to an ideal disordered configuration of maximum density, and atoms can move freely inside without change of energy[22]. Spaepen[23] presented a model which described the plastic flow and the evolution of free volume inside BMGs, namely free volume model. Based on free volume theory, the BMGs are in the metastable non-equilibrium structures. The internal atomic structure includes some excess free volume[24]. Generally, the increase in free volume reduces the material viscosity and leads to a drop in strength[25].

When a sample is annealed at elevated temperature, a relaxation process with structural rearrangement leads to an annihilation of free volume inside[26]. The structural rearrangement is the origin of spontaneous internal atomic ordering which entails reorganization of the constituent units over some larger length scale[27]. The reorganization of internal structure makes the excess free volume reduced or even completely annihilated, leading the internal enthalpy change and heat release[28,29]. Under the same heating condition, the unit of surface area can absorb a certain degree of energy. With the unified height-diameter ratio of 1.5, the specific surface area of different size samples can be calculated as follows:

$$S/V = \left(2\pi R^2 + 2\pi R \times 3R\right)/\left(\pi R^2 \times 3R\right) = 8/3R \qquad (2)$$

According to Eq. 2, with the sample size increasing, the specific surface area decreases. The energy per unit volume absorbed by the large sample is less than the small one, namely the larger sample has the lower heating efficiency. The DSC experiments have been carried out to check the internal enthalpy changes of different size annealed samples. Generally, the structural relaxation process occurs during the temperature range $(T_g - 200K \leq T \leq T_g)$, namely structural relaxed region[30]. In the structural relaxed areas, the annihilation of free volume leads heat releasing, as shown in Fig. 2. The relaxation enthalpy of larger sample is higher than smaller one. It indicates that the annihilation of free volume increases with the size increasing, namely the remaining free volume content of larger sample is higher than smaller one during the thermal process. Therefore, the larger specimen exhibits the lower flow stress, namely 'larger is softer'.

Meanwhile, the transition state theory based on the free volume model can also be used to explain the deformation mechanism of BMGs. In the case of compression tests, the constitutive relationship

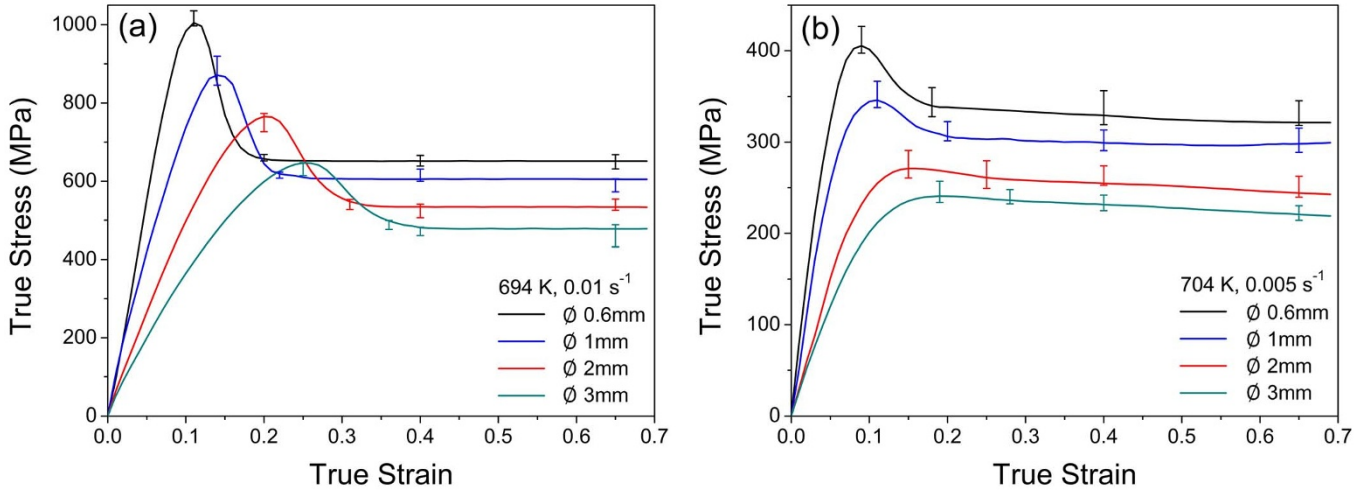

Figure 1 | The true stress–strain curves of Zr-based BMGs with different diameters at various conditions: (a) 694 K, 0.01 s^{-1}, (b) 704 K, 0.005 s^{-1}.

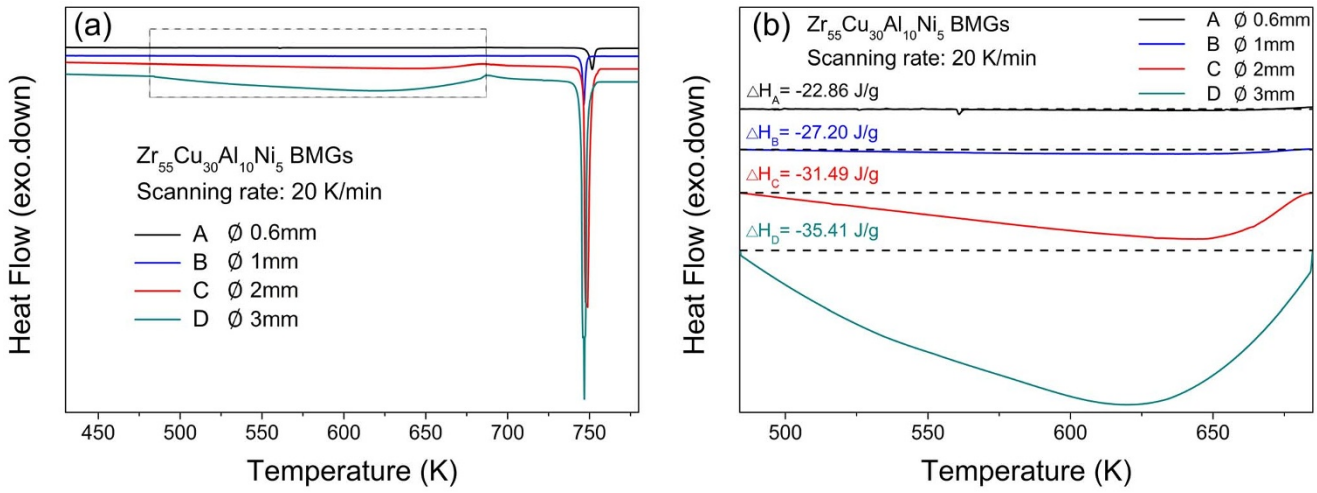

Figure 2 | The DSC curves of annealed $Zr_{55}Cu_{30}Al_{10}Ni_5$ BMGs with different diameters at a heating rate of 20 K/min. The baseline correction was conducted for all scans. Fig. b is the partial enlarged view of Fig. a.

between stress and strain rate is given by[31]:

$$\dot{\varepsilon} = \dot{\varepsilon}_0 sinh\left(\sigma V_{act} / \left(2\sqrt{3}kT\right)\right) \tag{3}$$

where V_{act} is the activation volume, exponential factor $\dot{\varepsilon}_0 = 2k_f c_f$ with c_f the defect concentration and k_f rate constant.

Figure 3 shows the activation volume and exponential factors of different sizes at four deformation temperatures. With size increasing, the activation volume of $Zr_{55}Cu_{30}Al_{10}Ni_5$ BMGs increases. Therefore, it could provide more free volume in order to satisfy the need of deformation. As is well known, the free volume is regarded as the elementary unit of plastic flow. The more activation volume, the plastic flow occurs more easily. On the other hand, the exponential factor increases with the size increasing, namely the defect concentration increases. More defect concentration provides more low strength regions, which is also beneficial for plastic deformation[32].

As mentioned above, we have proposed a Maxwell-pulse constitutive model (see Eq. 4) without considering the size effect to describe the stress-strain relationship[12]. This model can describe the steady stress and overshoot phenomenon during the deformation of a certain sized BMG sample in the SCLR. Thereby, we construct a size-dependent constitutive model which can well describe the deformation behavior of multi-scale samples based on this Maxwell-pulse type model.

$$\sigma = \sigma_f \left[1 - exp\left(\frac{-\varepsilon}{\tau_f \dot{\varepsilon}}\right)\right] + K\sigma_p \left[1 - exp\left(-\frac{\varepsilon}{t_1}\right)\right]^P exp\left(-\frac{\varepsilon}{t_2}\right) \tag{4}$$

where $\sigma_f = 3\dot{\varepsilon}Bexp\left(\frac{H}{RT}\right)\left\{1 - exp\left[-1/\left(tCexp\left(\frac{H^*}{RT}\right)\dot{\varepsilon}\right)\right]\right\}$ represents the steady stress, $\sigma_p = \dot{\varepsilon}exp\left(\frac{H'}{RT}\right)$ represents the overshoot peak stress and $\tau_f = \sigma_f/(3E\dot{\varepsilon})$ represents the stress relaxation time. All of the material parameters of $Zr_{55}Cu_{30}Al_{10}Ni_5$ BMG in the Maxwell-pulse constitutive model are listed in Table 1.

In order to describe the size effect of deformation behavior, the condition of sample size Ø1 mm, temperature 694 K and strain rate 0.01 s^{-1} under which the overshoot phenomenon is obvious, is chosen as the benchmark condition to analyze all the experiment data. The corresponding deformation variables are defined as d_0, T_0 and $\dot{\varepsilon}_0$. With sample size and temperature increasing and strain rate decreasing, the mechanical properties vary with the same trend. In other words, V, T and $1/\dot{\varepsilon}_0$ have similar influences on the variation tendency. These three variables can be normalized as follows:

$$S_V = V/V_0 = (d/d_0)^3 \tag{5}$$

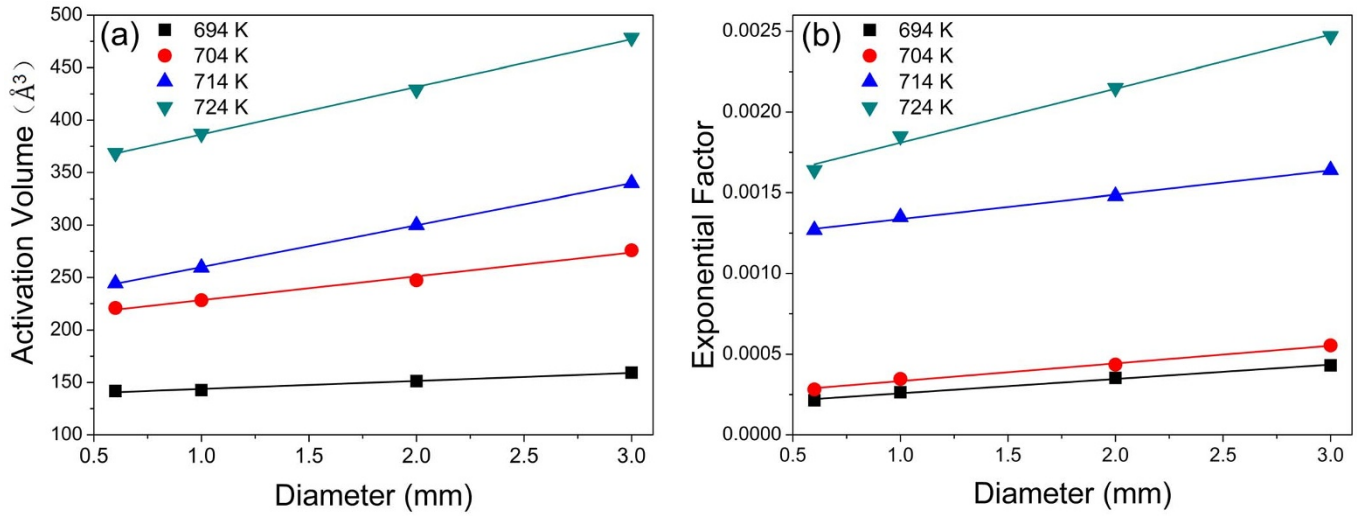

Figure 3 | (a) The activation volume V_{act}(Å^3) and (b) the exponential factor $\dot{\varepsilon}_0$ of different sizes at four deformation temperatures.

Table 1 | Material parameters of $Zr_{55}Cu_{30}Al_{10}Ni_5$ BMG

Parameter	Name
B	Structural constant
H	Flow stress activation energy
t	Relaxation time
C	Shift factor constant
*H**	Shift factor activation energy
K	Peak stress structural constant
t1	Forward half peak width
t2	Backward half peak width
P	Attenuation index
H′	Peak stress activation energy

$$S_T = T/T_0 \tag{6}$$

$$S_{\dot{\varepsilon}} = (1/\dot{\varepsilon})/(1/\dot{\varepsilon}_0) = \dot{\varepsilon}_0/\dot{\varepsilon} \tag{7}$$

where S_V, S_T and $S_{\dot{\varepsilon}}$ are the size, temperature and strain rate normalized factors, respectively.

From Figure 1, it can be intuitively observed that sample size mainly influence the following four physical properties: steady stress σ_f, elastic modulus E, overshoot peak stress σ_p and peak strain ε_p. Thus, the authors present four size-dependent factors, steady stress size-dependent factor $S_{\sigma f}$, elastic modulus size-dependent factor S_E, overshoot peak stress size-dependent factor $S_{\sigma p}$ and peak strain size-dependent factor $S_{\varepsilon p}$, to construct Maxwell-pulse type constitutive model for describing the size-dependent deformation behavior of BMGs in the SCLR. The size-dependent factor is expressed as a function of the normalized factors, as follows:

$$S = f(S_V, S_T, S_{\dot{\varepsilon}}) \tag{8}$$

The size-dependent factor $S_{\sigma f}$ is integrated into the first half part of Maxwell-pulse type model to describe the influence of sample sizes on steady stress. Because the first half part of Maxwell-pulse type model considers the effect of temperature and strain rate, only size normalized factor S_V is needed to model the size-dependent factor $S_{\sigma f}$ with respect to steady stress. According to the normalization method, $S_{\sigma f}$ can be defined as:

$$S_{\sigma f} = \sigma_f/\sigma_{f0} \tag{9}$$

where σ_{f0} is the steady stress corresponding to the benchmark condition. The steady flow behavior of BMGs can be analyzed in the framework of Weibull statistics[33,34]. The Weibull equation describes the transition probability P_f as a function of steady stress σ_f at a critical strain rate in form of:

$$P_f = 1 - exp\left[-V\left((\sigma_f - \sigma_z)/\sigma_0\right)^n\right] \tag{10}$$

where σ_0 is a scaling parameter, n is the Weibull modulus and V is the volume of BMGs sample, the parameter σ_z denotes the stress at which there is a zero transition probability, which is usually taken to be zero. Lee[33] deemed the characteristics viscous flows which cause transition can be assumed the same at a fixed transition probability. It means that P_f is constant. Adding variable d instead of V, Eq. 10 can be rewritten as:

$$d^3 \cdot {\sigma_f}^n = Const \tag{11}$$

The Weibull modulus n can be deduced by a logarithm transformation of Eq. 11 as follows:

$$ln\ \sigma_f = -3\ lnd/n + k \tag{12}$$

Plots of steady stress at a critical strain rate are shown in Figure 4. The well linear correlation between $ln\ \sigma_f$ and $ln\ d$ at Weibull modulus n = 14.4 indicates that the relationship between steady stress and sample size can be well described by the Weibull distribution in the experimental size range. So, $S_{\sigma f}$ can be expressed as follows by combining Eq. 9 and Eq. 11:

$$S_{\sigma f} = {S_V}^{-1/n} \tag{13}$$

Generally, the elastic modulus is derived mainly from two aspects: the atomic bonding strength and the possible dynamic relaxation of atomic structure[35]. Wang[36] indicated that the elastic modulus E is the macro measurement of the energy barrier ΔF for the linear elastic flow behavior. Under a stable thermodynamics condition, the energy barrier of each atomic bonding is almost identical. Because the defect concentration c_f in a large sample is higher than that in a small one (see Figure 3b), there are fewer atomic bonds in a unit volume of the large sample. That is to say, the energy barrier in a unit volume of the large sample is lower. Hence, ΔF shows a monotonic relationship with sample size.

From the energy landscape theory perspective[37], the elastic modulus E is associated with the activation energy density ρ_E which is defined as the energy barrier of a unit volume:

$$\rho_E = kE = \Delta F/V_m \tag{14}$$

where k is the function of Poisson's ratio v, V_m is the molar volume. Because parameter k of the same components BMG is a constant, ΔF is directly proportional to the elastic modulus E. Thus, the elastic modulus E also possesses a monotonic relationship with sample size in the SCLR. Given the relationship between elastic modulus and sample size is expressed:

$$E(V) = k_v V + b_v = k_v d^3 + b_v \tag{15}$$

where k_v represents the slope of the size variation of E and b_v is a constant.

Similarly, strain rate and temperature also influence the elastic modulus. Cao[38] proved that the reduction of elastic modulus is induced by decreasing strain rate. In addition, it is reported the variation of elastic modulus with strain rate is approximately linear[39]. Therefore, the relationship between elastic modulus and strain rate can be given as:

$$E(\dot{\varepsilon}) = k_{\dot{\varepsilon}}\dot{\varepsilon} + b_{\dot{\varepsilon}} \tag{16}$$

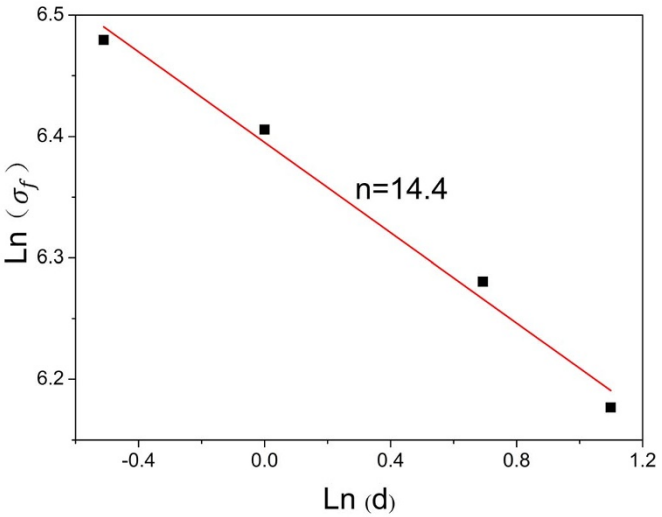

Figure 4 | The logarithmic relationship between steady stress and sample diameter.

where $k_{\dot{\varepsilon}}$ represents the slope of the strain rate variation of E and $b_{\dot{\varepsilon}}$ is a constant. Henann[40] indicates that the relationship between elastic modulus and temperature can be expressed as a type of hyperbolic tangent function:

$$E(T) = \frac{1}{2}(E_{max} + E_{min}) - \frac{1}{2}(E_{max} - E_{min}) * tanh\left(\frac{1}{\Delta E}(T - T_0)\right) - K_T(T - T_0) \quad (17)$$

where E_{max} and E_{min} are representative maximum modulus and minimum modulus of the experimental data, ΔE is a parameter denoting the difference between E_{max} and E_{min}, and K_T represents the slope of temperature variation of E.

Our interest here is developing a simple model which can reflect the size, strain rate and temperature influences on deformation behavior of BMGs. We construct the elastic modulus size-dependent factor S_E as:

$$S_E = k_1 * S_V + k_2 * S_{\dot{\varepsilon}} + k_3\left[\frac{1}{2E_0}(E_{max} + E_{min}) - \frac{1}{2E_0}(E_{max} - E_{min}) * tanh\left(\frac{T_0}{\Delta E}(S_T - 1)\right) - K_T T_0(S_T - 1)\right] + b \quad (18)$$

where k_1, k_2 and k_3 respectively represent the coordination coefficients of different variables, E_0 is the elastic modulus corresponding to the benchmark condition and b is a constant.

De Hey[41] have reported that under stable conditions, the rate of variation of defect concentration can be estimated as a balance between the generation induced by plastic strain and annihilation induced by structural relaxation. If a dynamical equilibrium defect concentration $c_{f,eq}$ is established, a constant steady-state stress is obtained. On the contrary, if the generation is less than the annihilation, the overshoot phenomenon occurs. Based on free volume theory, the overshoot phenomenon can be due to the variation of defect concentration[42]. The defect concentration c_f is given by[43]:

$$c_f = exp\left(-\gamma v^*/v_f\right) \quad (19)$$

where γ is a geometric factor, v_f is the mean free volume, i.e. the average excess volume per atom at a given temperature and v^* is the critical size for which an atomic jump can occur. Bletry indicates that the viscosity appears to be inversely proportional to the defect concentration, i.e. $\eta \propto C_f^{-1}$. In this approach, the lower defect concentration of BMGs leads to the higher viscosity. It means that the deformation behavior is more difficult of the small size, namely the small sample generates more distinct stress overshoot phenomenon than the large one. Therefore, the overshoot peak stress increases with the sample size decreasing, as shown in Figure 1. Meanwhile, assuming the mean free volume v_f of different sized samples is consistent, the critical size v^* decreases with the defect concentration increasing. It means that the free volume is more likely to be activated, to generate more activation volume. In terms of Bletry's research[44], the larger activation volume would lead to the wider amplitude of the overshoot peak. Therefore, a larger peak strain occurs in larger sample.

It can be known from the above paragraphs that the overshoot peak stress and peak strain are significantly influenced by the sample size. By adopting the least square method to analyze the experimental data, it is revealed that the relationship between the overshoot peak stress size-dependent factor and the normalized factors agrees well with the Arrhenius equation. So does the peak strain size-dependent factor. The temperature can be extracted from the Arrhenius equation during isothermal deformation. Thus, the comprehensive influences of deformation variables on the stress overshoot phenomenon can be described by the following equations:

$$S_{\sigma p}{}' = \sum [l_n * exp(q_n * S_n)] \quad (n = 1,2,3) \quad (20)$$

$$S_{\varepsilon p} = \sum [m_n * exp(p_n * S_n)] \quad (n = 1,2,3) \quad (21)$$

where l_n, q_n, m_n and p_n are structural constants, while S_1, S_2 and S_3 represent S_V, S_T and $S_{\dot{\varepsilon}}$ normalized factors respectively. However, the stress overshoot phenomenon is closely associated to the deformation modes[45]. Along with the transition from non-Newtonian flow to Newtonian flow, the stress overshoot phenomenon disappears. The overshoot peak stress size-dependent factor should be ignored. Therefore, a Max function combined with Eq. 20 is used to describe the existence or disappearance of the stress overshoot phenomenon, as follows:

$$S_{\sigma p} = Max\left\{0, S_{\sigma p}{}'\right\} \quad (22)$$

The four size-dependent factors mentioned above are integrated into the Maxwell-pulse type constitutive model:

$$\sigma = S_{\sigma f} \cdot \sigma_{f0}\left[1 - exp\left(\frac{-\varepsilon \cdot S_E}{S_{\sigma f} \cdot \tau_f \dot{\varepsilon}}\right)\right] + S_{\sigma p} \cdot K\dot{\varepsilon} exp\left(\frac{H'}{RT}\right)\left[1 - exp\left(-\frac{\varepsilon}{S_{\varepsilon p} \cdot t_1}\right)\right]^P exp\left(-\frac{\varepsilon}{S_{\varepsilon p} \cdot t_2}\right) \quad (23)$$

where $\sigma_{f0} = 3\dot{\varepsilon} B exp\left(\frac{H}{RT}\right)\left\{1 - exp\left[-1/\left(tC exp\left(\frac{H^*}{RT}\right)\dot{\varepsilon}\right)\right]\right\}$ and $\tau_f = \sigma_f/(3E_0\dot{\varepsilon})$.

Based on the size-dependent Maxwell-pulse type constitutive model, the true stress–strain curves of different sized BMG samples are fitted, as shown in Figure 5. The dashed lines represent the true stress–strain curves obtained from micro cylinder compression experiments while solid lines stand for the results predicted by the proposed constitutive model. It can be seen that the curves of the proposed constitutive model agree with those of experiment of BMGs in the SCLR. It also reproduces the size-dependent transition from non-Newtonian to Newtonian flow, which plays a key role in the application of BMGs in micro thermoplastic forming.

Finite element method (FEM) as a highly efficient calculation method, which is associated with equilibrium, geometrical and constitutive model, is widely used for analyzing the deformation process. The material constitutive model with or without size effect has a significant impact on the accuracy of the calculation. Correspondingly, the consistency between the calculated result and practical deformation process can certify the validation of proposed size-dependent constitutive model. A micro double cup extrusion process was conducted by FEM simulations and experiments. Two types of FEM simulations were carried out using commercially DEFORM software integrated with the proposed size-dependent constitutive model. One FEM simulation is based on the proposed model, and the other one is based on Maxwell-pulse model without size effect[12]. Figure 6a shows a 3D micrograph of the extruded double cup with an upper cup height of 1.26 mm and a sidewall thickness of 500 μm. Figure 6b and Figure 6c show the simulated geometry shape based on the constitutive models with or without size effect, respectively. From the comparison, it is obvious that the FEM simulation with the proposed size-dependent constitutive model can reproduce the double cup shape (with upper cup height of 1.28 mm) more accurately than that without size effect (with upper cup height of 1.32 mm). Furthermore, the overall shape simulated with the proposed constitutive model agrees better with the experimental results. The insert in Figure 6a is a partial enlarged view of the upper cup edge, while the blue line labeled as a is the experimental profile, the red line b and the black line c are the profiles simulated by the constitutive models

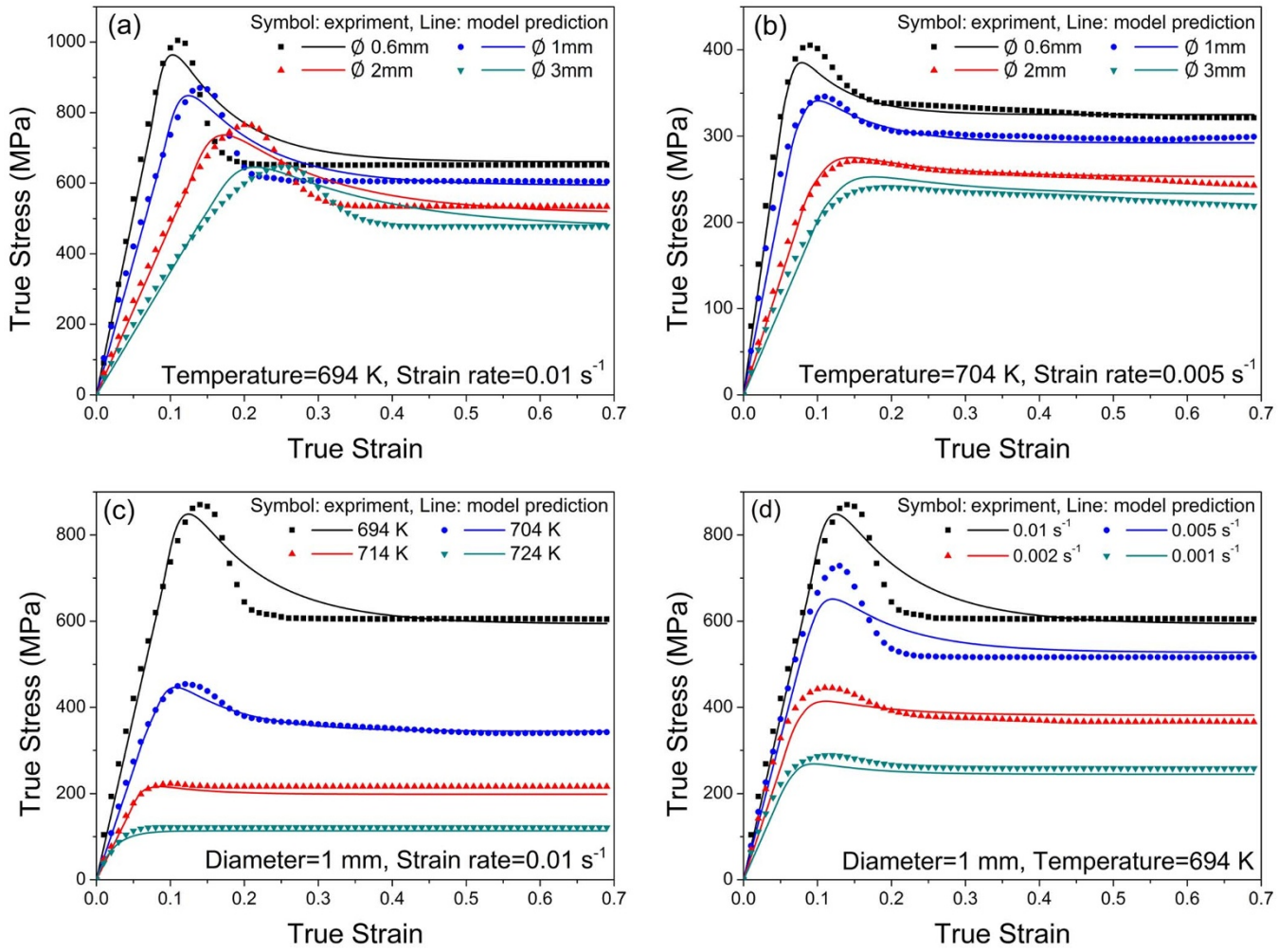

Figure 5 | Comparison of predicted results and experimental data (a) 694 K, 0.01 s^{-1}, and (b) 704 K, 0.005 s^{-1} with different sample sizes, (c) 1 mm, 0.01 s^{-1} at different temperatures (d) 1 mm, 694 K with different strain rates.

with and without size effect, respectively. It is obvious that the height difference of the inner wall (ΔH_{ab} = 38 μm) between the experiment (Figure 6a) and the simulation with size effect (Figure 6b) is much less than that (ΔH_{ac} = 140 μm) between the experiment and the simulation without size effect (Figure 6c). The Line b matches up better with the Line a, in comparison with the Line c. Therefore, it is proved that the proposed model can precisely predict the material flow behavior.

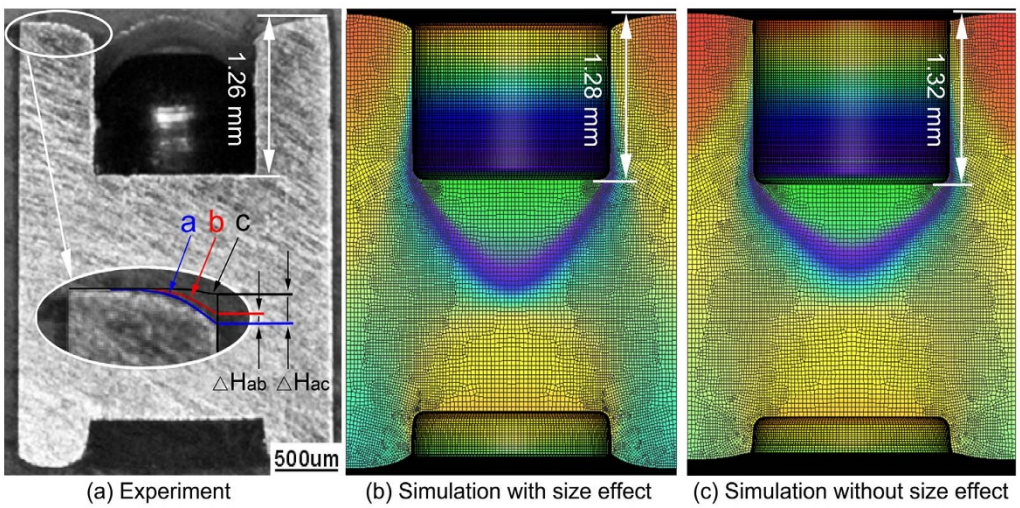

Figure 6 | Experimental and two simulated samples of the micro double cup extrusion. In partial enlarged view, the blue line a, the red line b and the black line c are the experimental profile and the simulated profiles, respectively.

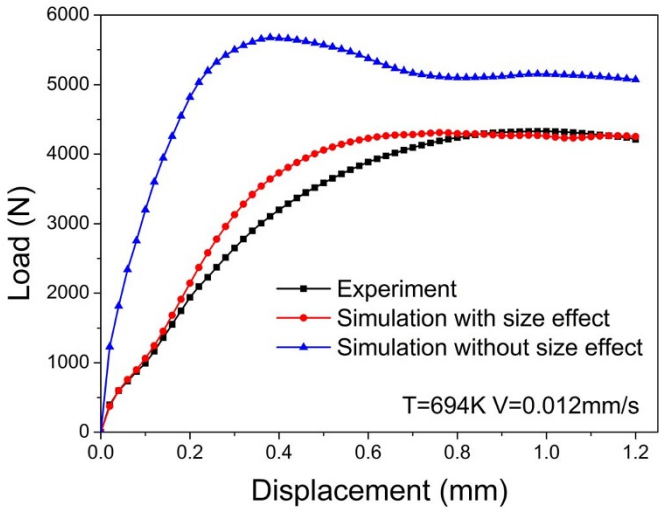

Figure 7 | Experimental and simulated load–displacement curves of the micro double cup extrusion.

In addition, Figure 7 shows the load–displacement curves of micro double cup extrusion experiment and corresponding simulations. It is clearly demonstrated that the load simulated with the proposed size-dependent constitutive model agrees well with experimental results. However, the load simulated with the constitutive model regardless of the size effect shows tremendous differences with the experimental result. Therefore, it is confirmed that the size-dependent constitutive model constructed by us is accurate. Generally, it is able to realize more accurate calculation during BMGs plastic deformation process in the SCLR when considering the size effect in FEM simulation.

In summary, the sample size has a significant effect on the deformation behavior of BMGs in the SCLR. It is found that larger samples exhibit lower flow stress through the uniaxial compression experiments of $Zr_{55}Cu_{30}Al_{10}Ni_5$ BMG. The variation of activation volume and defect concentration is utilized to provide a reasonable explanation of the size effect mechanism. In order to describe the deformation behavior of BMGs, a size-dependent Maxwell-pulse type constitutive model is established through integrating the size-dependent factors which reflect the influence of different deformation variables. The validated results reveal that the proposed size-dependent constitutive model can accurately predict the actual plastic deformation processes. Thus, the proposed size-dependent constitutive model is believed to provide accurate and effective foundation for the understanding of deformation behavior, as well as the further research of BMGs in the micro thermoplastic deformation.

Methods

The $Zr_{55}Cu_{30}Al_{10}Ni_5$ (atomic ratio) bulk metallic glass rod with a diameter of 3 mm was fabricated by arc-melting mixture of Zr, Al, Ni and Cu pure metals under a Ti-gettered argon atmosphere, followed by drop casting into copper molds. To minimize the initial free volume difference among different sized samples caused by different cooling rates during solidification, four size cylindrical samples (Ø0.6 mm, Ø1 mm, Ø2 mm and Ø3 mm) with an aspect ratio of 1.5 were precisely machined under water cooling from the as-cast Ø3 mm rods. Both end surfaces of the samples were polished carefully to make them parallel to each other and perpendicular to the longitudinal axis of samples.

The uniaxial compression tests were conducted at 694 K, 704 K, 714 K and 724 K with various strain rates (ranging from 1×10^{-3} s^{-1} to 1×10^{-2} s^{-1}) using a Zwick/Roell Z020 universal testing machine equipped with an air furnace. Graphite lubricant was used to reduce the friction between the end surfaces and anvil. The load and stroke were monitored and recorded automatically.

The isothermal annealing experiment was carried out by heating the cylindrical samples of different sizes at a heating rate of 100 K/min up to the desired temperature (694 K) and holding 3 minutes, then cooling rapidly down to room temperature. The thermal response of annealed samples was investigated with differential scanning calorimetry (DSC, Perkin–Elmer DSC-7) at a heating rate of 20 K/min. The baseline correction was conducted for all scans.

BMG samples for FEM simulations were symmetric about the y-axis with dimensions of Ø3 × 3 mm and divided into 6000 mesh elements in the half side of the sample due to symmetry. The deformation processes were conducted at 694 K in the SCLR with an extrusion rate of 0.012 mm/s. The simulations were performed up to 200 steps and completed at the extrusion stroke of 1.2 mm. The extrusion ratio was 0.36. Then a double-cup extrusion experiment of $Zr_{55}Cu_{30}Al_{10}Ni_5$ BMG was conducted under the same conditions as the FEM simulations on the Zwick/Roell Z020 universal testing machine.

1. Wu, F. F., Chan, K. C., Jiang, S. S., Chen, S. H. & Wang, G. Bulk metallic glass composite with good tensile ductility, high strength and large elastic strain limit. *Sci. Rep.* **4**, 5302 (2014).
2. Schroers, J. Processing of bulk metallic glass. *Adv. Mater.* **22**, 1566–1597 (2010).
3. Ketov, S. V. & Louzguine-Luzgin, D. V. Localized shear deformation and softening of bulk metallic glass: stress or temperature driven? *Sci. Rep.* **3**, 2798 (2013).
4. Saotome, Y., Itoh, K., Zhang, T. & Inoue, A. Superplastic nanoforming of Pd-based amorphous alloy. *Scripta Mater.* **44**, 1541–1545 (2001).
5. Evenson, Z., Raedersdorf, S., Gallino, I. & Busch, R. Equilibrium viscosity of Zr–Cu–Ni–Al–Nb bulk metallic glasses. *Scripta Mater.* **63**, 573–576 (2010).
6. Csach, K., Fursova, Y. V., Khonik, V. A. & Ocelik, V. Non-Newtonian plastic flow of a Ni-Si-B metallic glass at low stresses. *Scripta Mater.* **39**, 1377–1382 (1998).
7. Kato, H., Kawamura, Y., Inoue, A. & Chen, H. S. Newtonian to non-Newtonian master flow curves of a bulk glass alloy $Pd_{40}Ni_{10}Cu_{30}P_{20}$. *Appl. Phys. Lett.* **73**, 3665 (1998).
8. Kawamura, Y., Nakamura, T., Kato, H., Mano, H. & Inoue, A. Newtonian and non-Newtonian viscosity of supercooled liquid in metallic glasses. *Mater. Sci. Eng. A* **304**, 674–678 (2001).
9. Johnson, W. L., Lu, J. & Demetriou, M. D. Deformation and flow in bulk metallic glasses and deeply undercooled glass forming liquids—a self consistent dynamic free volume model. *Intermetallics* **10**, 1039–1046 (2002).
10. Lu, J., Ravichandran, G. & Johnson, W. L. Deformation behavior of the $Zr_{41.2}Ti_{13.8}Cu_{12.5}Ni_{10}Be_{22.5}$ bulk metallic glass over a wide range of strain-rates and temperatures. *Acta Mater.* **51**, 3429–3443 (2003).
11. Seop Kim, H., Kato, H., Inoue, A. & Chen, H.-S. Finite element analysis of compressive deformation of bulk metallic glasses. *Acta Mater.* **52**, 3813–3823 (2004).
12. Wang, X. Y. *et al.* A Maxwell-pulse constitutive model of $Zr_{55}Cu_{30}Al_{10}Ni_5$ bulk metallic glasses in supercooled liquid region. *J. Alloys Compd.* **509**, 2518–2522 (2011).
13. Jun, H. J., Lee, K. S., Yoon, S. C., Kim, H. S. & Chang, Y. W. Finite-element analysis for high-temperature deformation of bulk metallic glasses in a supercooled liquid region based on the free volume constitutive model. *Acta Mater.* **58**, 4267–4280 (2010).
14. Anand, L. & Su, C. A constitutive theory for metallic glasses at high homologous temperatures. *Acta Mater.* **55**, 3735–3747 (2007).
15. Anand, L. & Su, C. A theory for amorphous viscoplastic materials undergoing finite deformations, with application to metallic glasses. *J. Mech. Phys. Solids* **53**, 1362–1396 (2005).
16. Huang, Y. J., Shen, J. & Sun, J. F. Bulk metallic glasses: Smaller is softer. *Appl. Phys. Lett.* **90** (2007).
17. Zheng, Q., Cheng, S., Strader, J. H., Ma, E. & Xu, J. Critical size and strength of the best bulk metallic glass former in the Mg–Cu–Gd ternary system. *Scripta Mater.* **56**, 161–164 (2007).
18. Li, N., Li, D. J., Wang, X. Y. & Liu, L. Size-dependent flowing characteristics of a Zr-based bulk metallic glass in the supercooled liquid region. *J. Alloys Compd.* **523**, 146–150 (2012).
19. Wang, X. Y., Deng, L., Tang, N. & Jin, J. S. Size Effect on Flow Behavior of a $Zr_{55}Al_{10}Ni_5Cu_{30}$ Bulk Metallic Glass in Supercooled Liquid State. *Metall. Mater. Trans. A* **45A**, 3505–3511 (2014).
20. Jiang, Q. K. *et al.* Super elastic strain limit in metallic glass films. *Sci. Rep.* **2**, 852 (2012).
21. Shao, Z. *et al.* Size-dependent viscosity in the super-cooled liquid state of a bulk metallic glass. *Appl. Phys. Lett.* **102** (2013).
22. Cohen, M. H. & Turnbull, D. Molecular Transport in Liquids and Glasses. *J. Chem. Phys* **31**, 1164 (1959).
23. Spaepen, F. A microscopic mechanism for steady state inhomogeneous flow in metallic glasses. *Acta Metall.* **25**, 407–415 (1977).
24. Khonik, V. A., Kosilov, A. T., Mikhailov, V. A. & Sviridov, V. V. Isothermal creep of metallic glasses: a new approach and its experimental verification. *Acta Mater.* **46**, 3399–3408 (1998).
25. Spaepen, F. Homogeneous flow of metallic glasses: A free volume perspective. *Scripta Mater.* **54**, 363–367 (2006).
26. Schuh, C. A., Hufnagel, T. C. & Ramamurty, U. Overview No.144 - Mechanical behavior of amorphous alloys. *Acta Mater.* **55**, 4067–4109 (2007).
27. Schall, P., Weitz, D. A. & Spaepen, F. Structural rearrangements that govern flow in colloidal glasses. *Science* **318**, 1895–1899 (2007).
28. Altounian, Z. Reversible structural relaxation in metallic glasses. *Mater. Sci. Eng.* **97**, 461–468 (1988).
29. Liu, X., Liu, X. & Altounian, Z. Formation and thermal stability of an $E9_3$-structured $NiHf_2$ phase in $Ni_{33}Hf_{67}$. *Acta Mater.* **53**, 1439–1447 (2005).

30. Chen, H. S. Kinetics of low temperature structural relaxation in two (Fe-Ni) based metallic glasses. *J. Appl. Phys.* **52**, 1868–1870 (1981).
31. Wang, Q., Pelletier, J. M., Blandin, J. J. & Suery, M. Mechanical properties over the glass transition of $Zr_{41.2}Ti_{13.8}Cu_{12.5}Ni_{10}Be_{22.5}$ bulk metallic glass. *J. Non-Cryst. Solids* **351**, 2224–2231 (2005).
32. Liu, Y. H. *et al*. Super plastic bulk metallic glasses at room temperature. *Science* **315**, 1385–1388 (2007).
33. Lee, C. J., Huang, J. C. & Nieh, T. G. Sample size effect and microcompression of $Mg_{65}Cu_{25}Gd_{10}$ metallic glass. *Appl. Phys. Lett.* **91**, 161913 (2007).
34. Velázquez-Ortega, L. & Rodríguez-Romo, S. Local effective permeability distributions for non-Newtonian fluids by the lattice Boltzmann equation. *Chem. Eng. Sci.* **64**, 2866–2880 (2009).
35. Huo, L. S., Zeng, J. F., Wang, W. H., Liu, C. T. & Yang, Y. The dependence of shear modulus on dynamic relaxation and evolution of local structural heterogeneity in a metallic glass. *Acta Mater.* **61**, 4329–4338 (2013).
36. Wang, W. H. The elastic properties, elastic models and elastic perspectives of metallic glasses. *Prog. Mater Sci.* **57**, 487–656 (2012).
37. Debenedetti, P. G. & Stillinger, F. H. Supercooled liquids and the glass transition. *Nature* **410**, 259–267 (2001).
38. Cao, Q. P. *et al*. Bending behavior of electrodeposited glassy Pd–P and Pd–Ni–P thin films. *Scripta Mater.* **68**, 455–458 (2013).
39. Chabrier, F., Lloyd, C. H. & Scrimgeour, S. N. Measurement at low strain rates of the elastic properties of dental polymeric materials. *Dent. Mater.* **15**, 33–38 (1999).
40. Henann, D. & Anand, L. A constitutive theory for the mechanical response of amorphous metals at high temperatures spanning the glass transition temperature: Application to microscale thermoplastic forming. *Acta Mater.* **56**, 3290–3305 (2008).
41. De Hey, P., Sietsma, J. & Van Den Beukel, A. Structural disordering in amorphous $Pd_{40}Ni_{40}P_{20}$ induced by high temperature deformation. *Acta Mater.* **46**, 5873–5882 (1998).
42. Bletry, M., Guyot, P., Blandin, J. J. & Soubeyroux, J. L. Free volume model: High-temperature deformation of a Zr-based bulk metallic glass. *Acta Mater.* **54**, 1257–1263 (2006).
43. Heggen, M., Spaepen, F. & Feuerbacher, M. Creation and annihilation of free volume during homogeneous flow of a metallic glass. *J. Appl. Phys.* **97**, 033506 (2005).
44. Bletry, M., Guyot, P., Brechet, Y., Blandin, J. J. & Soubeyroux, J. L. Transient regimes during high-temperature deformation of a bulk metallic glass: A free volume approach. *Acta Mater.* **55**, 6331–6337 (2007).
45. Lee, K. S. & Chang, Y. W. Extrusion formability and deformation behavior of $Zr_{41.2}Ti_{13.8}Cu_{12.5}Ni_{10}Be_{22.5}$ bulk metallic glass in an undercooled liquid state after rapid heating. *Mater. Sci. Eng. A* **399**, 238–243 (2005).

Acknowledgments

This research was financially supported by the National Natural Science Foundation of China (Grant No. 51175202) and the New Century Talent Supporting Project (Grant No. NCET-11-0185). The authors are also grateful for the technical assistance from the Analytical and Testing Center of HUST and the Analytical Platform of the State Key Laboratory of Materials Processing and Die & Mould Technology.

Author contributions

D.Y., L.D. and X.Y.W. designed the study. D.Y., M.Z. and N.T. conducted the experiments and FEM simulation. D.Y. analyzed the data. D.Y., L.D. and X.Y.W. constructed the size-dependent constitutive model. D.Y., L.D., M.Z., X.Y.W. and J.J.L. wrote the manuscript.

Additional information

Competing financial interests: The authors declare no competing financial interests.

How to cite this article: Di Yao *et al*. A size-dependent constitutive model of bulk metallic glasses in the supercooled liquid region. *Sci. Rep.* **5**, 8083; DOI:10.1038/srep08083 (2015).